2.B: 2.L

Nuclear Physics A297 (1978) 189–205; © *North-Holland Publishing Co., Amsterdam*

SCATTERING OF POLARIZED ^{3}He BY ^{4}He BETWEEN 18 AND 32 MeV

Y.-W. LUI, O. KARBAN, A. K. BASAK †, C. O. BLYTH, J. M. NELSON and S. ROMAN

Department of Physics, University of Birmingham, England

Received 4 November 1977

Abstract: Analysing power angular distributions for elastic scattering of ^{3}He by ^{4}He have been measured between 18 and 32 MeV in 2 MeV steps. The data together with differential cross sections were analysed in terms of the standard phase-shift formalism. A new level with a $J^\pi = \frac{1}{2}^-$ assignment was established at 16.7 MeV excitation energy in ^{7}Be and described using the R-matrix single-level formula. The phase-shift behaviour in this energy region is discussed and compared with predictions of resonating-group theory.

E NUCLEAR REACTIONS ^{4}He($\vec{^3}$He, ^{3}He), E = 18–32 MeV; measured $A(\theta)$; deduced phase shifts. ^{7}Be deduced level J, π.

1. Introduction

The structure of the ^{7}Be nucleus has been extensively studied in a number of experiments involving ^{3}He-^{4}He and p-^{6}Li scattering and its low-lying levels are well established and understood. For the ^{3}He-^{4}He case, differential cross section measurements and phase-shift analysis from 5 to 18 MeV (all energies refer to $E_{^3\mathrm{He}}$(lab)) have been reported by Spiger and Tombrello [1]), who also measured cross sections of the ^{4}He(^{3}He, p)^{6}Li reaction populating the ground and first excited states in ^{6}Li. Accurate measurements of the differential cross section in 2 MeV steps between 17.8 and 30 MeV have been performed by Jacobs and Brown [2]). Schwandt *et al.* [3]) measured the differential cross section of elastic scattering of ^{3}He by ^{4}He in the energy range between 27.2 and 43 MeV and also investigated the behaviour of the phase shifts in this energy range.

Double-scattering experiments to study the polarization in ^{3}He-^{4}He elastic scattering at 7.8, 8.3, 8.8 and 13 MeV have been reported by Armstrong *et al.* [4]) and at energies of 11.5 and 12.85 MeV by McEver *et al.* [5]). Hardy *et al.* [6]) used a polarized ^{3}He target to obtain polarization excitation functions at 79.3 and 114.0° (c.m.) between 5.7 and 13.5 MeV ^{3}He energy. These data, together with the double-scattering results, were later analyzed using the phase-shift formalism by Hardy *et al.* [7]). The polarized target measurements have been recently extended to higher

† Present address: Physics Department, Rajshahi University, Rajshahi, Bangladesh.

energies by Bacher *et al.* [8]) who obtained polarization data at five scattering angles between 18.4 and 31.8 MeV of the corresponding ^{3}He energy.

For the p-^{6}Li scattering, the ground-state differential cross section data were obtained between 2.4 and 12 MeV by Harrison and Whitehead [9]), while for the 2.18 and 3.56 MeV states results below 9.5 MeV were reported by Harrison [10,11]). Polarization measurements and phase-shift analysis have been performed by Brown and Petitjean [12]).

As a result of these experiments, many levels of ^{7}Be below an excitation energy of 11 MeV have been established [1,11,12]). However, above 18 MeV ^{3}He energy, discontinuities exist in the phase shifts deduced from the cross section measurements and only very limited polarization data are available. As the Birmingham polarized ^{3}He beam has a maximum energy of 33.3 MeV, it is possible to form the ^{7}Be compound system up to 20 MeV excitation energy. Thus it is of considerable interest to study this virtually unknown region of polarization and to investigate the level structure

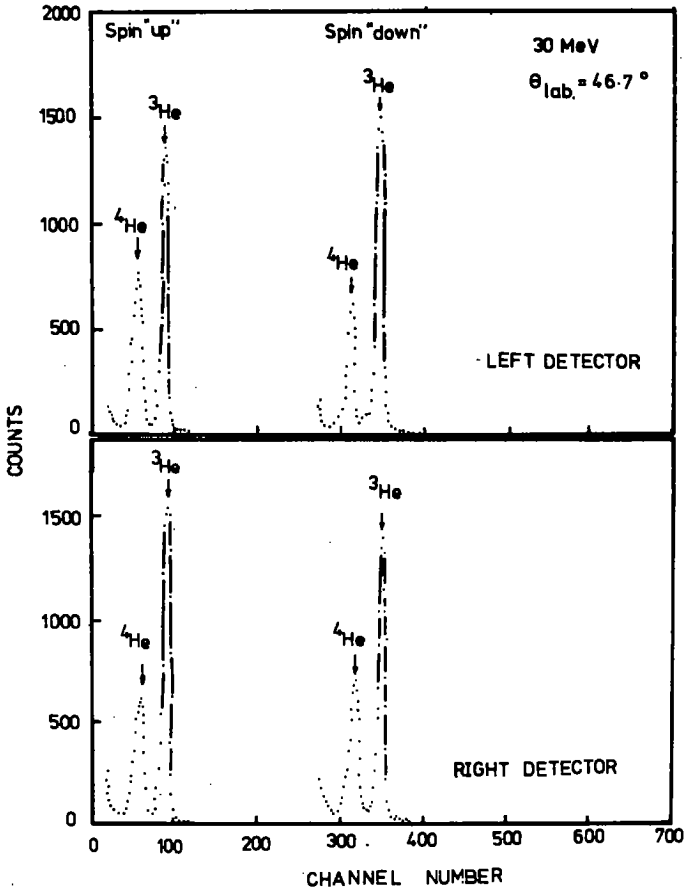

Fig. 1. The energy spectra of ^{3}He and recoil ^{4}He particles without particle identification.

of ^{7}Be between 11 and 20 MeV excitation energy. An additional reason for measuring the analysing powers in the 18–33 MeV region was to explore the possibility of employing the ^{3}He-^{4}He scattering in a polarimeter for a polarized ^{3}He beam. Regions of high polarization varying smoothly with energy and angle were reported by Armstrong *et al.* [4]) and consequently used in polarimeters designed for double-scattering experiments [5, 13]).

2. Experiment and results

The ^{3}He analysing power angular distributions between 18 and 32 MeV were measured using the 33.3 MeV polarized ^{3}He beam accelerated in the Radial Ridge Cyclotron of the University of Birmingham. The beam has an on-target intensity of 0.5 nA and a polarization of $P_b = 0.38$. The sign of the beam polarization was changed between positive and negative values approximately every 2 sec by a small

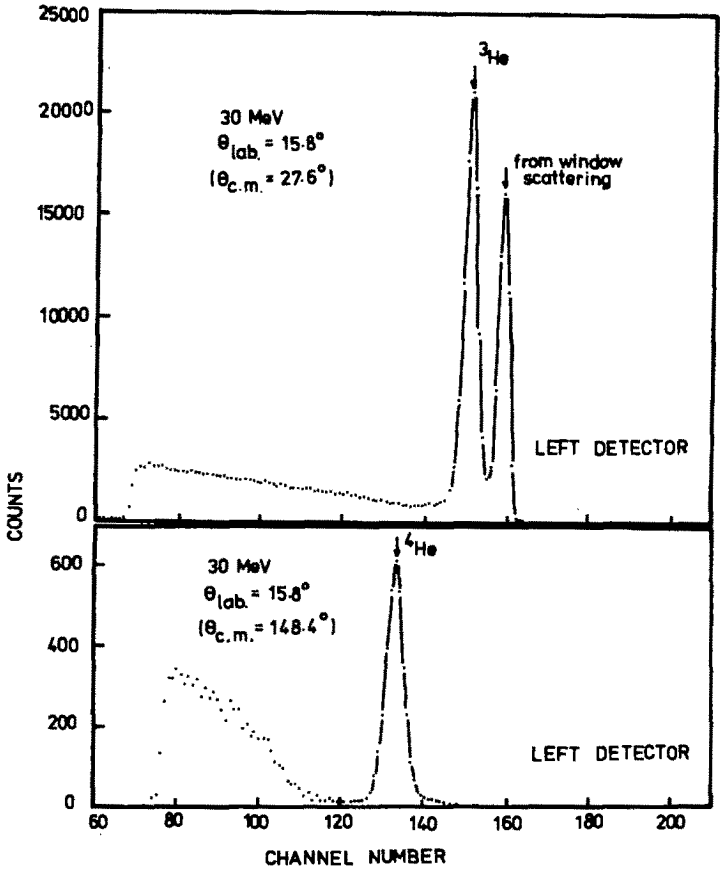

Fig. 2. The energy spectra of ^{3}He and recoil ^{4}He particles with particle identification. The low-energy cut-off corresponds to energies at which the particle does not emerge from the ΔE counter.

transverse magnetic field acting on the metastable $^3He^+$ ions before ionization and injection. A polarimeter [14]) based on ^3He-^2H scattering was used to monitor the beam polarization during a run.

A cylindrical gas cell [15]) containing the natural helium gas under a pressure of 2 atm was used to scatter the polarised ^3He particles. Aluminium foils placed in front of the gas cell were used to degrade the beam energy to the required value. The thickness of the foil for each energy, together with the energy loss in the Havar cell window, were determined using the tables of ref. [16]). The total energy spread including the target thickness and the energy straggling varied between 0.2 MeV at 32 MeV and 0.6 MeV at 18 MeV. The lowest energy accessible by this technique was limited by the energy of recoil ^4He particles emerging from the gas cell, which prevented a full angular distribution being obtained at energies overlapping with the data of Hardy *et al.* [7]).

Both scattered and recoil particles were detected simultaneously in six ΔE-E

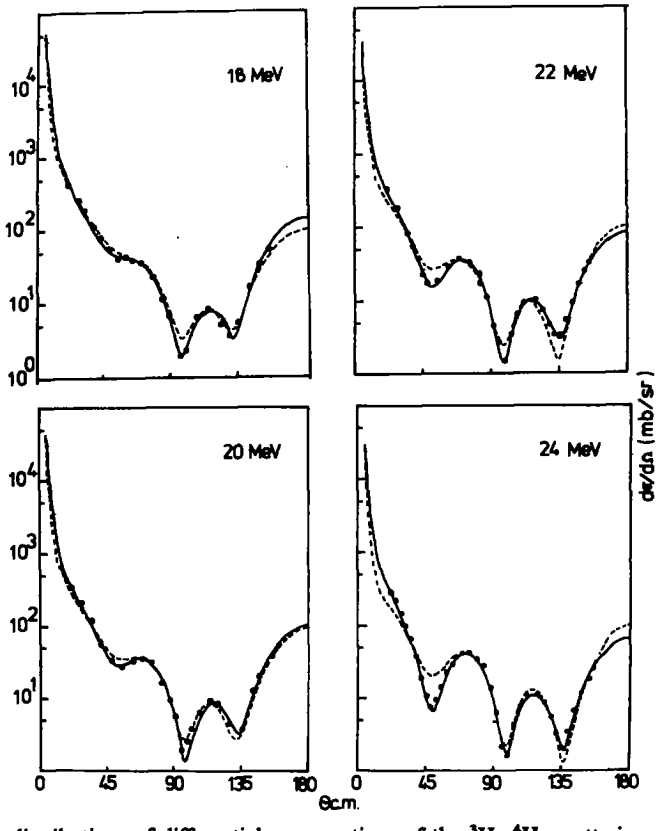

Fig. 3. Angular distributions of differential cross sections of the ^3He-^4He scattering at 18, 20, 22 and 24 MeV [the data are taken from ref. [2])]. The dashed curves represent predictions of the resonating-group theory the solid curves are results of the phase-shift analysis, solution C.

silicon surface-barrier detector telescopes situated at three symmetric scattering angles on the left and right of the beam line. The particle identification system was not used at scattering angles where the detected particle range was less than 150 μm. Instead, the detector thickness was kept as small as possible by regulating the bias across the detector in order to clean the spectra from charge-1 particles (fig. 1). The separation of mass-4 and mass-3 particles was, however, essential at small scattering angles where the corresponding yields differ significantly (fig. 2). Some amount of window scattering at these angles did not interfere with the ^{3}He peak corresponding to the scattering by ^{4}He, as shown in fig. 2. The data acquisition system, formulae for extraction of analysing power values and other experimental details are given in ref. [17]).

The experimental analysing powers cover an angular range from 27.6° to 150° in the c.m. system and an energy range from 18 to 32 MeV in 2 MeV steps. The statistical errors for most of the data are less than 0.05 except for some points near 100° which are associated with a sharp minimum in the differential cross section (figs. 3 and 4), where the error is about 0.10. The triangular points, plotted with the

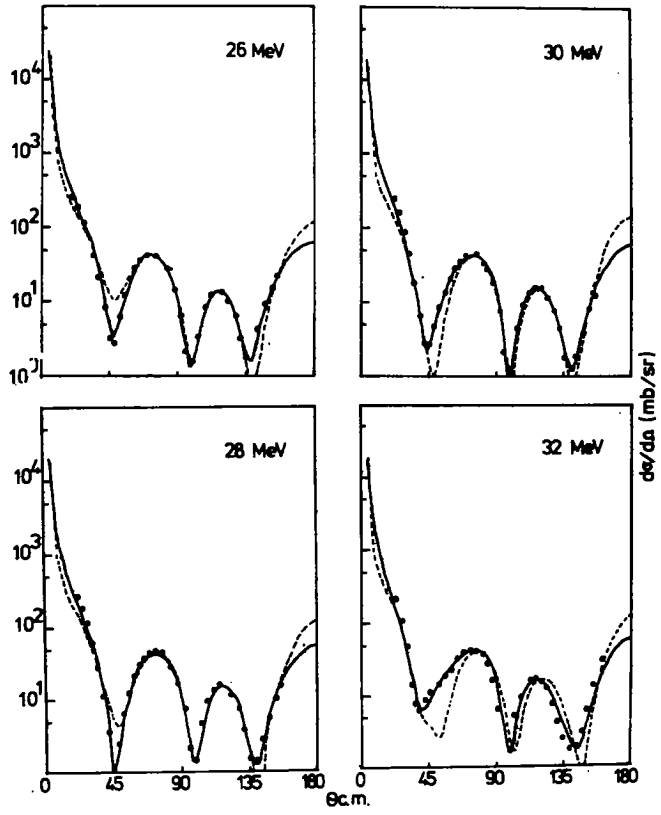

Fig. 4. Angular distributions of differential cross sections of the ^{3}He-^{4}He scattering at 26, 28, 30 and 32 MeV [the data are taken from ref. [2])]. See caption to fig. 3.

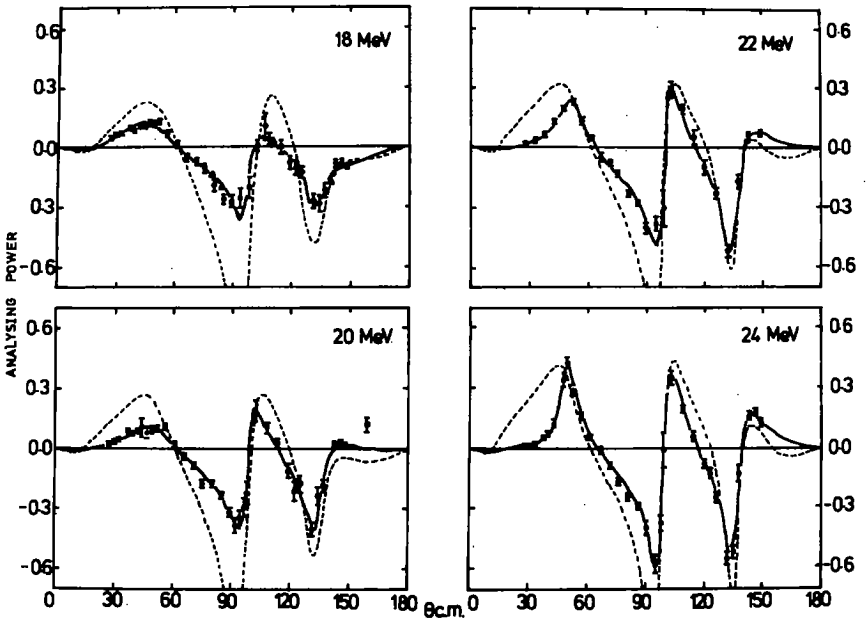

Fig. 5. Analysing power angular distributions of the ^{3}He-^{4}He scattering at 18, 20, 22 and 24 MeV. See caption to fig. 3.

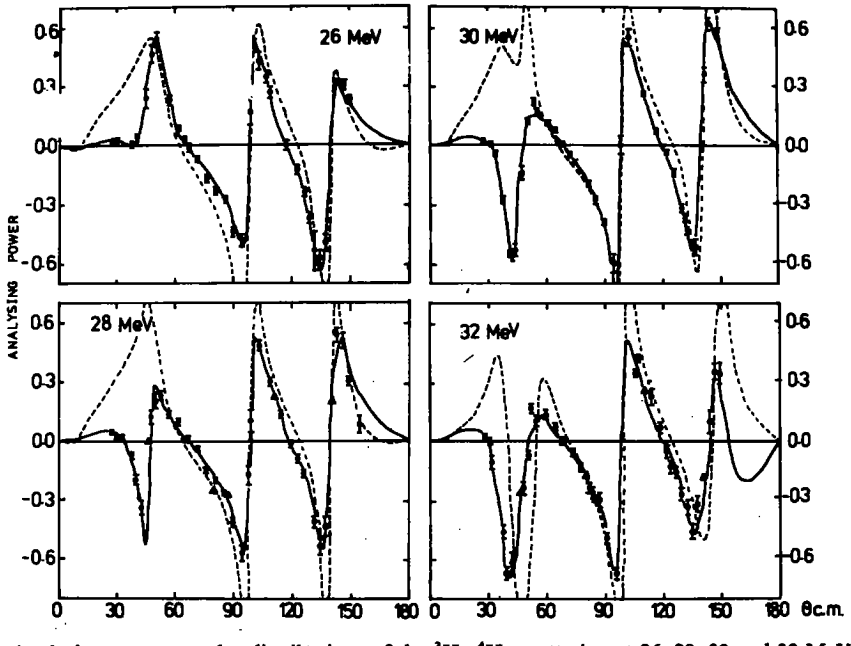

Fig. 6. Analysing power angular distributions of the ^{3}He-^{4}He scattering at 26, 28, 30 and 32 MeV. See caption to fig. 3.

present analysing powers in figs. 5 and 6, were obtained by Bacher *et al.* [8]) using the polarized ^{3}He target. Although their data are taken at slightly different energies the agreement with the present results is very good.

The main features of the experimental analysing power are the decrease in magnitude with decreasing energy, the disappearance of the 40° minimum between 26 and 28 MeV, and less rapid changes between positive and negative extrema of the angular distributions at lower energies. While there is no obvious resonant behaviour of the cross section data, the analysing powers, when plotted as an excitation function, e.g. at 50° (c.m.) reveal a broad resonant-like structure around 25 MeV (fig. 7).

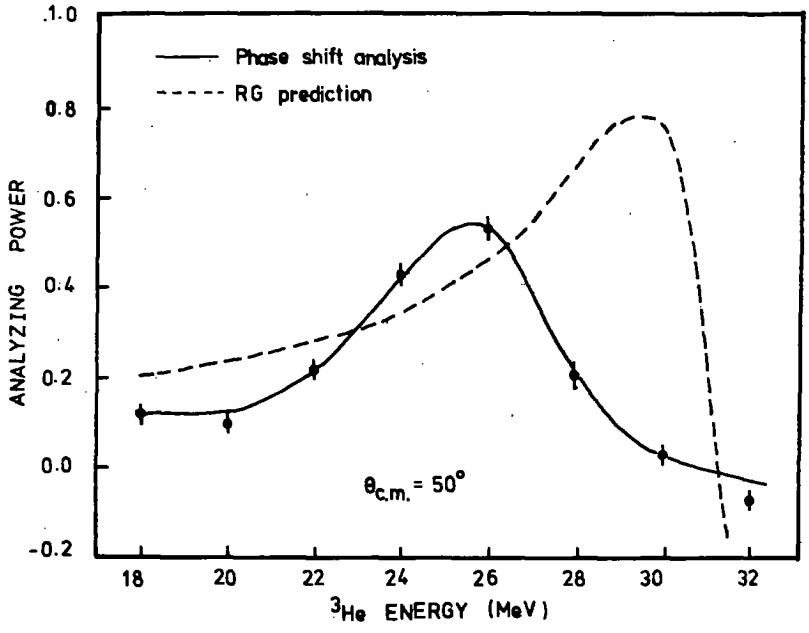

Fig. 7. Analysing power excitation function at 50° (c.m.). See caption to fig. 3.

3. The phase-shift analysis

A standard phase-shift formalism for the scattering of spin-$\frac{1}{2}$ particles on spin-zero nuclei [1]) was employed to analyse the experimental data. The present analysing power results together with the differential cross section data from literature [2, 3]) were fitted simultaneously by an automatic search routine minimising the χ^2 function [1]).

Since in the present experiment the ^{7}Be compound system can be formed at high excitation energy, some of the reaction channels, such as p+^{6}Li and d+^{5}Li are energetically open. All these channels should be taken into account and this can be

done formally by allowing the phase shifts to become complex [1]), i.e.

$$\delta_l \rightarrow \delta_l^{\mathrm{R}} + i\delta_l^{\mathrm{I}},$$

$$\exp(2i\delta_l) \rightarrow \exp(2i\delta_l^{\mathrm{R}} - 2\delta_l^{\mathrm{I}}). \tag{1}$$

Alternatively, we can define $\exp(-2\delta_l^{\mathrm{I}}) = \cos^2 X_l$, where the latter term is usually called the absorption coefficient. Then we can replace $\exp(i\delta_l)\sin\delta_l$ by

$$[\cos^2 X_l \exp(2i\delta_l^{\mathrm{R}})\sin\delta_l^{\mathrm{R}} + i\{\tfrac{1}{2}(1-\cos^2 X_l)\}],$$

or

$$\tfrac{1}{2}i\{1-\cos^2 X_l \exp(2i\delta_l^{\mathrm{R}})\}. \tag{2}$$

The search routine allowed up to ten parameters to be varied simultaneously.

It is well known that the results of a phase-shift analysis may depend on the initial values and also on the first few sub-searches. Thus it was necessary to establish first a search procedure which would give the fastest convergence of the χ^2 function. Then the groups of parameters searched on in each sub-search and the sequence of sub-searches were kept identical at each energy in order to eliminate further uncertainties. Starting from the top or bottom energy, the solution was used as an initial set at the next energy. The searches were terminated when the change in χ^2 value was less than 1 %. Only solutions giving a smooth and continuous energy dependence of the phase shifts were considered. With these restrictions three solutions were found, depending on the starting set of phase shifts, which are referred to as solution A, B and C.

Solution A. The search was started using the parameters of Spiger and Tombrello [1]) for 18 MeV as the initial values, fitting the 18 MeV differential cross section data only. After the χ^2 minimum was reached the resulting set of phase shifts was used as a starting point in searches to fit the differential cross section and analysing power data simultaneously. When the solution at 18 MeV was found the search continued at other energies as described above.

Solution B. The initial set was obtained using results of the optical-model analysis [18]) of the differential cross section and analysing power at 32 MeV. The search was carried out from 32 to 18 MeV.

Solution C. The searches were started from phase shifts predicted by the resonating group theory at 18 MeV. The theoretical values were obtained by Furber [19]) for the energy range 1.7–44.5 MeV in calculations with a two-nucleon spin-orbit term in the intercluster potential generating split phase shifts. When these phase shifts were used directly as starting points at each energy the search results were practically the same as those obtained from the above procedure.

The χ^2 values per point averaged over all energies for the solutions A, B and C are 2.43, 2.28 and 2.19, respectively. Most of the real phase shifts are accurate to $\pm 3°$ and the imaginary phase shifts to $\pm 5°$. This means that when changing the phase

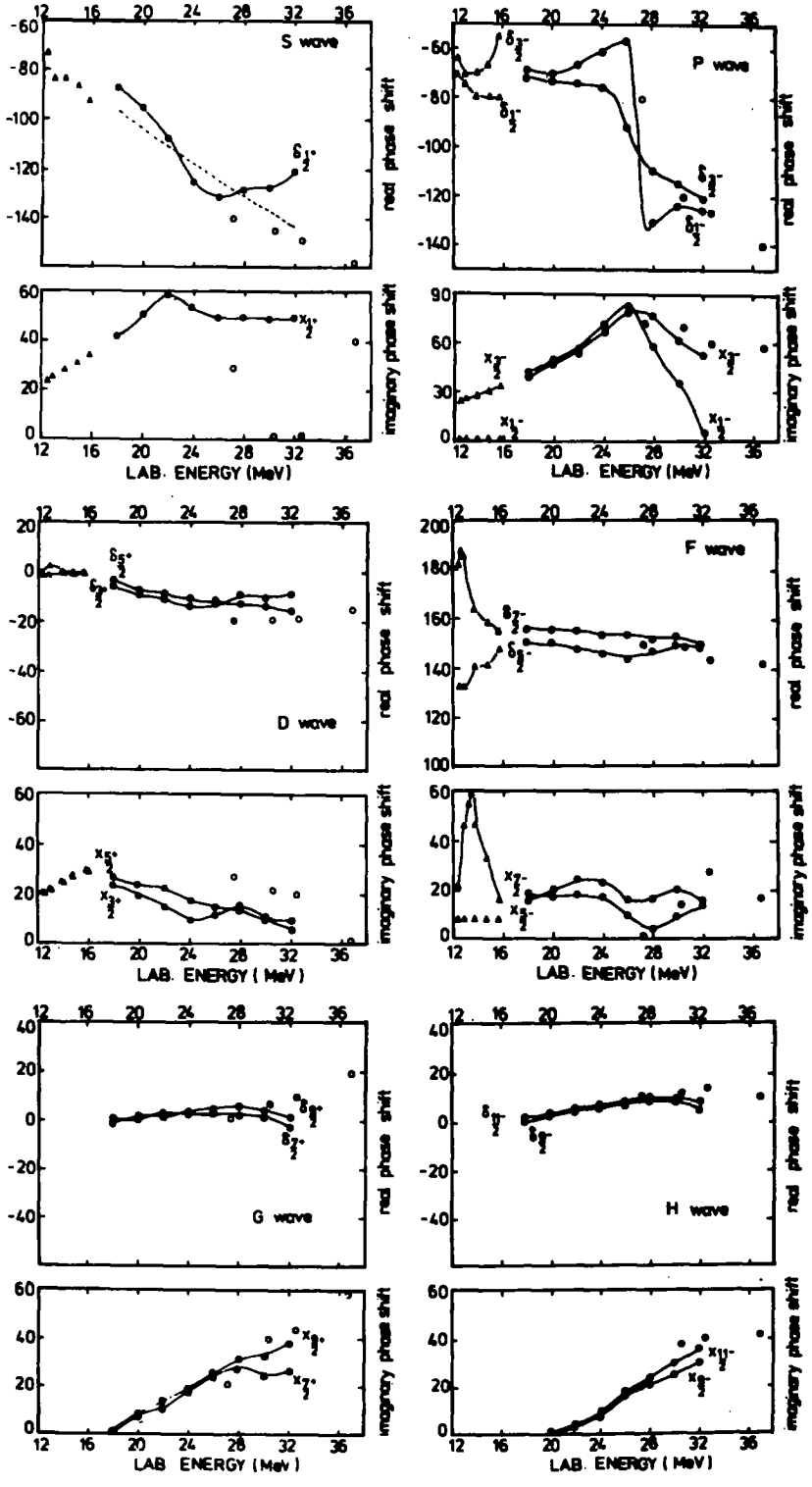

Fig. 8. The ^{4}He(^{3}He, ^{3}He)^{4}He phase shifts (solution C) in degrees showing the S-, P-, D-, F-, G- and H-wave phase shifts as a function of energy. The symbols are explained in the text.

shifts by this amount, the χ^2 values increase by about 50 % with respect to the best-fit value. It is evident that all three solutions give equally good fits to the data and the quality of the agreement is independent of energy. The maximum l-value used in the calculations vary from $l = 4$ at 18 MeV to $l = 7$ at 32 MeV. Predictions for differential cross sections and analysing powers obtained with the solution C are shown as solid lines in figs. 3–7. Predictions with solutions A and B deviate from the solid lines practically only at angles where no experimental data exist and they are not shown in the figures.

4. Behaviour of the phase shifts

Several sets of phase shifts deduced from the analysis of ^{3}He-^{4}He scattering data have been reported in the literature between 5 MeV and 43 MeV ^{3}He energy, namely the split phase shifts from 5 MeV to 18 MeV of Spiger and Tombrello [1]) obtained from the differential cross section data only, and the split phase shifts between 5.69 and 15.87 MeV deduced by Hardy *et al.* [7,20]) using both differential cross section and polarization data. Unsplit phase shifts at six energies between 27.2 and 43 MeV were reported by Schwandt *et al.* [3]). Thus the present work fills the existing gap between 18 and 27.2 MeV and it is interesting to check how the above solutions A, B and C match the earlier results. The main differences between these three solutions are in the S-, P- and D-waves. For the higher l-values the phase-shift values are similar. Since it is impractical to show phase shifts for all three solutions, only results of solution C (full circles) are plotted in fig. 8. These are compared with results of refs. [7,20]) and ref. [3]) which are shown as triangles and open circles respectively. The behaviour of the phase shifts and their features for individual partial waves are discussed below. The notation $\delta_{j\pi}$ and $X_{j\pi}$ with $j = l \pm \frac{1}{2}$, $\pi = (-)^l$ is used.

The S-wave phase shifts. The $\delta_{\frac{1}{2}+}$ phase shifts of solutions C and A have similar energy dependence while that of solution B remains about constant. At low energy, solution C matches reasonably well with the results of refs. [1,7]), while at high energy, there is a noticeable discrepancy with ref. [3]). The same is true for the imaginary phase shifts. The slope of the $\delta_{\frac{1}{2}+}$ energy dependence can be averaged (dotted line) by the hard-sphere phase shifts calculated with a radius 2.4 fm. No levels associated with the S-wave were found in this energy interval.

The P-wave phase shifts. In solution C, the resonance behaviour of the $\delta_{\frac{1}{2}-}$ phase shift together with a maximum in the $X_{\frac{1}{2}-}$ phase shift around 27 MeV indicate an assignment of $\frac{1}{2}^-$ for a level in ^{7}Be at about 16.7 MeV. The value of $\delta_{\frac{1}{2}-}$ shown at 26 MeV has a large uncertainty because of the large absorption that takes place at this energy ($X_{\frac{1}{2}-} \approx 82°$). The $X_{\frac{1}{2}-}$ also has a maximum at 26 MeV but the behaviour of $\delta_{\frac{1}{2}-}$ provides insufficient evidence to be interpreted as a $\frac{3}{2}^-$ resonance. In solution A, the splitting between $\delta_{\frac{1}{2}-}$ and $\delta_{\frac{1}{2}-}$ becomes large around 26 MeV. Both the $X_{\frac{1}{2}-}$ and $X_{\frac{1}{2}-}$ phase shifts have large values and the $X_{\frac{1}{2}-}$ phase shift goes through a maximum between 24 and 26 MeV. However, the anomalous behaviour of the

$l = 1$ phase shifts in solution A is difficult to interpret by any parameters of the one-level R-matrix formula. The real $l = 1$ phase shifts in solution B have a monotonic energy dependence but the $X_{\frac{1}{2}^-}$ becomes large at 26 MeV. Only $l = 1$ phase shifts of solution C match those of ref. [3]). In contrast to results of refs. [1,7]), the value of $X_{\frac{1}{2}^-}$ is close to $X_{\frac{1}{2}}$ at 18 MeV.

The D-wave phase shifts. The splitting of the real phase shifts in solution C reverses sign near 27 MeV. The $X_{\frac{3}{2}^+}$ phase shift shows some structure near 28 MeV while the $X_{\frac{5}{2}^+}$ phase shift varies smoothly over this energy range. Solution A is similar to solution C. In solution B the shape of the phase shifts is different. The small splitting between the real phase shifts at high energies become large at low energies. Both solution A and C can be matched to the results of refs. [1,3,7]).

The F-wave phase shifts. In solution C the real phase shifts are smooth in this energy region and are in good agreement with the results of refs. [3,1,7]). The imaginary phase shifts indicate some fluctuation which may be due to some inaccuracies in the data. Behaviour of solution A is essentially the same as solution C, but solution B is different and cannot match the results of refs. [1,3,7]).

Higher-wave phase shifts. The $l = 4$ to 7 real phase shifts of all solutions remain small over this energy range. The large values of the $l = 4$ and 5 imaginary phase

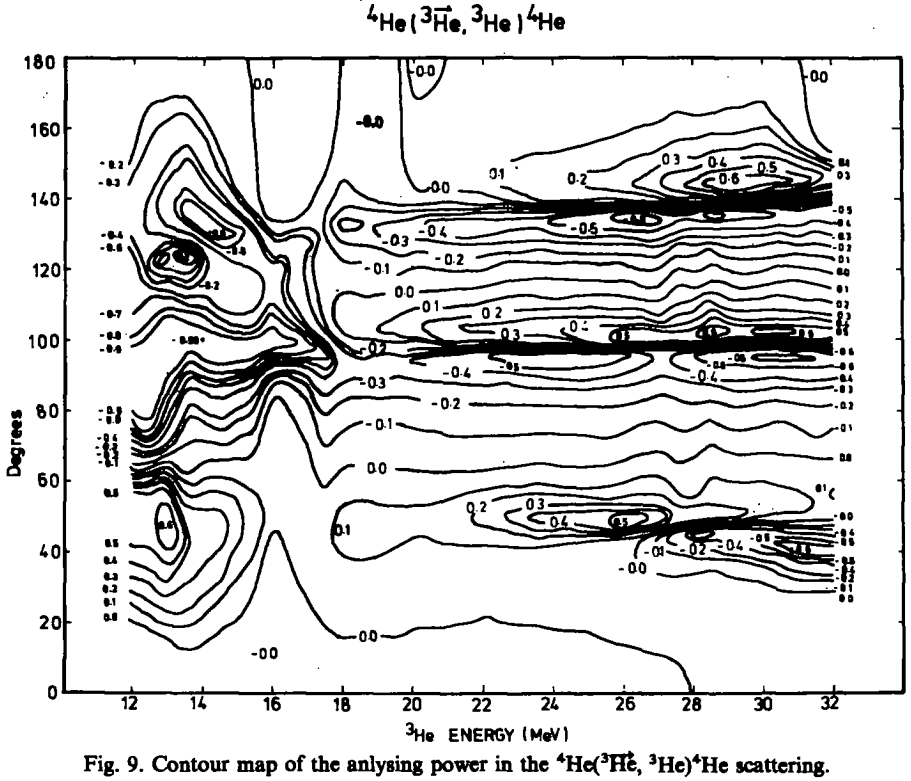

Fig. 9. Contour map of the anlysing power in the ^{4}He($^3\vec{H}$e, ^{3}He)^{4}He scattering.

shifts may be associated with three- and many-body break-up at higher energies. The $l = 6$ and 7 imaginary phase shifts of solutions A and B are zero at low energies and increase gradually, starting at 28 MeV. In solution C these imaginary phase shifts remain practically zero even above 28 MeV.

The polarization in the ^{4}He(^{3}He, ^{3}He)^{4}He scattering is shown as a contour plot in fig. 9. The analysing powers between 12.0 and 15.9 MeV were calculated from the phase shifts obtained by Hardy *et al.* [7,20]) and those between 18 and 32 MeV were obtained from the phase shifts of solution C of the present analysis. The predictions between 16 and 18 MeV were calculated using phase shifts corresponding to an interpolation between the above two sets. The contour map shows two regions of high analysing power at angles around 100° and 140° (c.m.) extending from 22 to 32 MeV. It also demonstrates the sharp angular dependence in the vicinity of these maxima and minima. The change of polarization sign between 26 and 28 MeV associated with the 27 MeV anomaly is clearly seen around 40° (c.m.).

5. Theoretical predictions

5.1. THE *R*-MATRIX THEORY

The application of *R*-matrix theory to the extraction of parameters of the suggested $\frac{1}{2}^-$ level was based on the simplified formalism given, e.g. by Bacher [21]). The total real phase shift δ deduced in the above analysis consists of the hard-sphere component ϕ and the resonant phase shift. The real part β and the imaginary part X of the resonant phase shift are given by expressions

$$\beta = \tfrac{1}{2}\tan^{-1}\left\{\frac{(E_r - E)\Gamma_e}{(E_r - E)^2 + \frac{1}{4}\Gamma^2 - \frac{1}{2}\Gamma_e\Gamma}\right\},$$

$$X = \cos^{-1}\left\{\frac{[(E_r - E)^2 + \frac{1}{4}\Gamma^2 - \frac{1}{2}\Gamma_e\Gamma]^2 - [(E_r - E)\Gamma_e]^2}{[(E_r - E)^2 + \frac{1}{4}\Gamma^2]^2}\right\}^{\frac{1}{2}},$$

where Γ_e is the elastic width, Γ is the total width, $E_r = E_{\lambda l} + \Delta_{\lambda l}$, E_r is the resonance energy, $E_{\lambda l}$ is the level energy and $\Delta_{\lambda l}$ is the level shift.

Thus, the real part of the resonant phase shift is not necessarily passing through $\frac{1}{2}\pi$ at the resonance energy and depends on the ratio of the elastic width to the total width. For $\Gamma_e/\Gamma < \frac{1}{2}$, the resonance phase shift has a maximum below E_r, a minimum above E_r and passes through zero at E_r. The potential scattering in this analysis was calculated using the interaction radius $r = 2.9$ fm. A limited search in the level parameters to fit the phenomenological phase shifts resulted in the following values: the elastic width $\Gamma_e = 3.2$ MeV, the total width $\Gamma = 6.5$ MeV and the resonance energy $E_r = 26.4$ MeV. The total phase shifts, which include both phase shifts from the potential scattering and the resonance predicted with these parameters, are compared with the phenomenological ones in fig. 10.

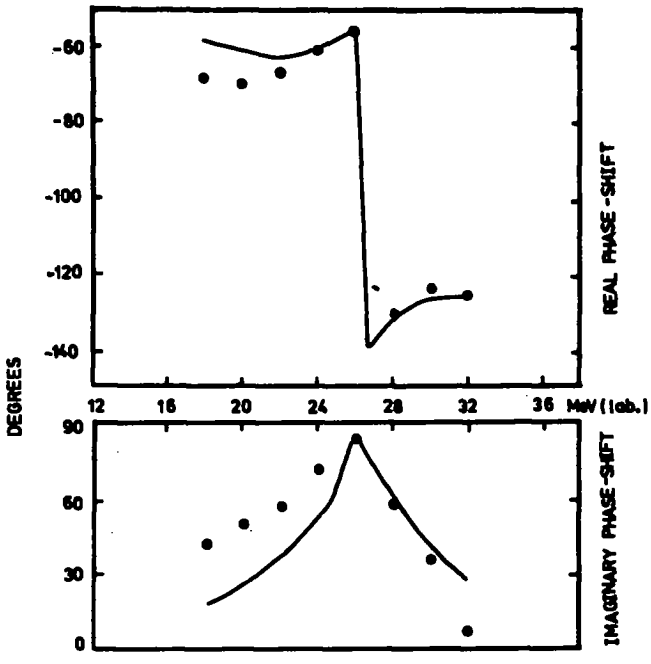

Fig. 10. The $\frac{1}{2}^-$ phase shifts (solution C) fitted with the one-level R-matrix formula.

The agreement between the real phase shifts is quite good except at low energies where the prediction of R-matrix theory lies above the phenomenological phase shifts. For the imaginary phase shifts, the magnitude is not in good agreement at lower energies but the shape of the energy dependence is reproduced. The deviation of both the real and imaginary phase shifts at low energies may be due to the choice of the interaction radius and also to the background contribution, since the latter was neglected in the analysis.

5.2. RESONATING-GROUP PREDICTIONS

The differential cross sections and analysing powers of ^{3}He-^{4}He scattering in the 18–32 MeV interval were calculated using theoretical phase shifts obtained by Tang and Furber [19]. In the resonating-group calculations the potential contained a spin-orbit term and a phenomenological imaginary term. The predictions are compared with the experimental data for cross sections in figs. 3 and 4, and for analysing powers in figs. 5, 6 and 7.

The theoretical phase shifts show no resonant behaviour between 18 and 32 MeV. The real phase shifts vary smoothly with energy and the imaginary phase shifts given by resonating-group theory for S- and P-waves are small compared with the results of the present analysis.

The agreement between the cross sections predicted by the resonating-group theory and the experimental ones is quite good. The analysing power data are reasonably well reproduced in the backward hemisphere, however the theory fails to follow the analysing power behaviour between 26 and 30 MeV and also overestimates the magnitude in the forward hemisphere.

5. Discussion

Both solutions A and C exhibit a resonance effect in the P-wave and indeed the shapes of the other phase shifts are similar. Phase shifts of solution B differ from the above two both in shape and magnitude. This fact cannot, however, be entirely associated with the optical-model starting values since after a few initial searches the phase shifts significantly departed from the starting parameters. Although all three solutions satisfy the criteria specified in sect. 3, further selection is possible by comparison with theoretical predictions. From this point of view, solution C is clearly favoured as it closely resembles the phase shifts predicted by the resonating-group method. A preference for solution C is further supported by the smallest χ^2 value and rapid convergence of the searches.

Difficulties connected with a substantial energy degradation of the incident

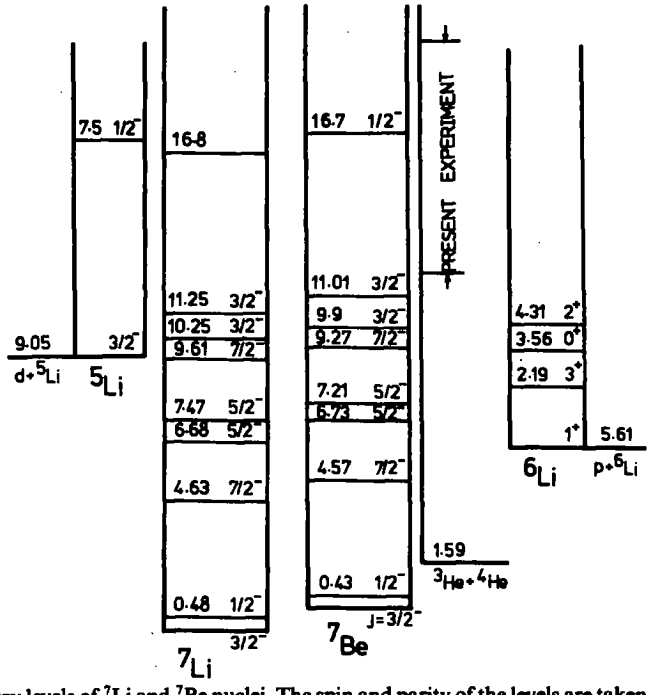

Fig. 11. Energy levels of ^{7}Li and ^{7}Be nuclei. The spin and parity of the levels are taken from ref. [22]).

33.3 MeV ^{3}He beam prevented measurements of the analysing power in the 15–18 MeV interval, which led to discontinuities in the phase shifts deduced in refs. [1,7,20]) and in the present work. The incorrect predictions of the analysing power by Spiger and Tombrello [1]) at 18 MeV stress again the danger of using phase shifts deduced from fits to the cross section data only to calculate the analysing powers.

The present phase-shift analysis revealed the anomalous behaviour of the $\frac{1}{2}^-$ phase shifts, both real and imaginary, which can be associated with a level in the compound system ^{7}Be. Using the *R*-matrix representation of the phenomenological phase shifts, the new $\frac{1}{2}^-$ level lies at 16.7 MeV excitation energy and has the ratio of the elastic to total width $\Gamma_e/\Gamma = 0.49$. This $\frac{1}{2}^-$ level could be interpreted as an analog to the 16.8 MeV level in ^{7}Li (see fig. 11 and ref. [22])) established by Rybka and Katz [23]). Recently, measurements of proton elastic and inelastic differential cross section and polarization for p-^{6}Li scattering were reported by Nelson *et al.* [24]). Their preliminary results indicate a presence of a broad resonance in ^{7}Be at a proton energy of 14 MeV, which corresponds to 17.6 MeV excitation energy in ^{7}Be.

The interpretation of the behaviour of the $\frac{3}{2}^-$ phase shifts is not so obvious since it depends on the treatment of the background phase shifts. The d + ^{5}Li* (first excited state) channel is open at 26.2 MeV ^{3}He energy. If there is a $\frac{3}{2}^-$ level then the resonance energy is very close to the threshold of this reaction channel. In such a case the state may be predominantly a d + ^{5}Li configuration and a strong coupling to the reaction channel takes place. Therefore the behaviour of the resonant phase shift will be changed by including the resonant background. Interference of these could strongly affect the behaviour of both the real and imaginary phase shifts and two-channel *R*-matrix formulae would be required for such an analysis. The latter, however, cannot be attempted without sufficient experimental information on the above reaction channel.

The phase shifts obtained from the resonating-group calculations and used to generate the predictions shown as dashed lines in figs. 3–7, were based on the one-channel (elastic) approximation of this method. Therefore, at higher energies when the reaction channels are open, this theoretical approach becomes less powerful. The non-elastic channels are taken into account by a phenomenological imaginary potential which cannot reflect individual characteristics of each channel. In spite of these approximations the theoretical curves represent remarkably well most of the experimental features. The present phase-shift analysis also showed that the theoretical set of phase shifts is best suited to provide starting values in the search procedure.

Attempts to calculate higher energy levels of the ^{7}Be nucleus using nuclear models such as the shell model, are very limited. The early shell-model prediction available between 11 and 19 MeV excitation has been calculated by Norton and Goldhammer [25]). The authors suggest two $\frac{1}{2}^-$ levels with isospin $\frac{1}{2}$ at 11.30 and 12.52 MeV and a $\frac{3}{2}^-$ level with isospin $\frac{1}{2}$ at 15.87 MeV. A $\frac{1}{2}^-$ level with isospin $\frac{3}{2}$ is predicted at 17.38 MeV and two $\frac{5}{2}^-$ levels at 13.4 and 15.85 MeV with isospin $\frac{1}{2}$ and $\frac{3}{2}$, respectively.

Recently, Irvine *et al.* [26]) performed shell-model calculations for a number of light nuclei. These calculations are based on the Reid soft-core interaction and supplement the shell-model wave function by introducing the strong two-body correlations via a Jastrow-type cluster expansion. The result for ^{7}Be nucleus shows that all the low-lying states are in good agreement with the experimental level scheme. In the energy interval of the present measurements, a $\frac{5}{2}^-$ level around 15 MeV, two $\frac{1}{2}^-$ levels and one $\frac{3}{2}^-$ level around 16.5 MeV, all with isospin $\frac{1}{2}$, were predicted. The present $\frac{1}{2}^-$ level at 16.7 MeV is therefore in good agreement with this shell-model calculation. However, in order to search for the other two suggested levels with small energy separation, more detailed and accurate experimental information is necessary in the 24–30 MeV region, including measurements of the reaction channels.

Finally, the measured analysing powers between 18 and 32 MeV indicate that the ^{3}He-^{4}He scattering in this energy region is not particularly suited for use in a polarimeter, in contrast to the situation near 13 MeV [ref. [4])]. For an efficient polarimeter it is necessary to have a high and constant analysing power over a wider range of energies and angles combined with a large cross section. The large analysing powers measured around 100 and 140° c.m. angles are accompanied by a rapid angular variation and occur at the cross section minima. The 40° c.m. negative minimum at higher energies would be apparently the best choice for a polarimeter based on the ^{3}He-^{4}He scattering. However, a comparison with the ^{3}He-^{2}H scattering data shows [14]) that the efficiency of a polarimeter using the latter is higher approximately by an order of magnitude.

The authors are indebted to Professor Tang for providing the resonating-group phase shifts prior to publication and to Professor Burcham and Professor Morrison for their interest in this work and critical discussions of the results.

References

1) R. J. Spiger and T. A. Tombrello, Phys. Rev. **163** (1967) 964
2) C. G. Jacobs, Jr., and R. E. Brown, Phys. Rev. **C1** (1970) 1615
3) P. Schwandt, B. W. Ridley, S. Hayakawa, L. Put and J. J. Kraushaar, Phys. Lett. **30B** (1969) 30
4) D. D. Armstrong, L. L. Catling, P. W. Keaton, Jr., and L. R. Veeser, Phys. Rev. Lett. **23** (1969) 135
5) W. S. McEver, T. B. Clegg, J. M. Joyce, E. J. Ludwig and R. L. Walter, Phys. Lett. **31B** (1970) 560
6) D. M. Hardy, R. J. Spiger, S. D. Baker, Y. S. Chen and T. A. Tombrello, Phys. Lett. **31B** (1970) 355
7) D. M. Hardy, R. J. Spiger, S. D. Baker, Y. S. Chen and T. A. Tombrello, Nucl. Phys. **A195** (1972) 250
8) A. D. Bacher, S. D. Baker, E. K. Biegert, D. P. May and E. P. Chamberlain, Proc. 4th Symp. on polarization phenomena in nuclear reactions (Birkhauser Verlag, Basel, 1976) p. 583
9) W. D. Harrison and A. B. Whitehead, Phys. Rev. **132** (1963) 2607
10) W. D. Harrison, Nucl. Phys. **A92** (1967) 253
11) W. D. Harrison, Nucl. Phys. **A92** (1967) 260
12) L. Brown and C. Petitjean, Nucl. Phys. **A117** (1968) 343;
C. Petitjean, L. Brown and R. G. Seyler, Nucl. Phys. **A129** (1969) 209
13) W. S. McEver, T. B. Clegg, J. M. Joyce, E. J. Ludwig and R. L. Walter, Nucl. Phys. **A178** (1972) 529;
E. J. Ludwig, T. B. Clegg and R. L. Walter, Nucl. Phys. **A211** (1973) 559
14) O. Karban, C. O. Blyth, Y.-W. Lui and S. Roman, Nucl. Instr. **141** (1977) 387

15) R. C. Brown, J. A. R. Griffith, O. Karban, L. Mesko, J. M. Nelson and S. Roman, **A207** (1973) 456
16) C. F. Williamson, J. P. Boujot and J. Picard, CEA report no. R3042 (1966), unpublished
17) W. E. Burcham, J. B. A. England, R. G. Harris, O. Karban and S. Roman, Nucl. Phys. **A246** (1975) 269
18) O. Karban *et al.*, J. of Phys. **G3** (1977) 571
19) Y. C. Tang and R. D. Furber, private communication
20) D. M. Hardy, Ph.D. thesis, Rice University, 1970, unpublished
21) A. D. Bacher, Cross-section and polarization studies of light nuclei, in Nuclear spectroscopy and reactions, part A (Academic Press, NY, 1974)
22) F. Ajzenberg-Selove and T. Lauritsen, Nucl. Phys. **A227** (1974) 1
23) T. W. Rybka and L. Katz, Phys. Rev. **110** (1958) 1123
24) C. E. Nelson *et al.*, Bull. Am. Phys. Soc. **22** (1977) 551
25) J. L. Norton and P. Goldhammer, Nucl. Phys. **A165** (1971) 33
26) J. M. Irvine, G. S. Mani, V. F. E. Pucknell, M. Vallieres and F. Yozici, preprint DL/NSF/P20, 1975, Daresbury Laboratory (unpublished)